Supplemental Materials for 'Multipolar Phase Transition in a $4f^2$ fcc Lattice Compound $PrCdNi_4$'

Yuka Kusanose,[1,2,*] Yasuyuki Shimura,[1] Kazunori Umeo,[3] Naomi Kawata,[3] Toshiro Takabatake,[1] Taichi Terashima,[4] Naoki Kikugawa,[5] Takako Konoike,[4] Yuya Hattori,[5] Kazuhiro Nawa,[6] Hung-Cheng Wu,[6,†] Taku J. Sato,[6] and Takahiro Onimaru[1]

[1]*Department of Quantum Matter, Graduate School of Advanced Science and Engineering, Hiroshima University, Higashi-Hiroshima 739-8530, Japan*

[2]*Department of Applied Physics, Nagoya University, Nagoya 464-8603, Japan*

[3]*Natural Science Center for Basic Research and Development (N-BARD), Hiroshima University, Higashi-Hiroshima 739-8526, Japan*

[4]*Research Center for Materials Nanoarchitectonics (MANA), National Institute for Materials Science (NIMS), Tsukuba 305-0003, Japan*

[5]*Center for Basic Research on Materials (CBRM), National Institute for Materials Science (NIMS), Tsukuba 305-0003, Japan*

[6]*Institute of Multidisciplinary Research for Advanced Materials, Tohoku University, Sendai 980-8577, Japan*

(Dated: March 24, 2025)

I. SAMPLE CHARACTERIZATION

Backscattered electron images and powder x-ray diffraction patterns for samples A and B of polycrystalline $PrCdNi_4$ are shown in Figs. S1 and S2, respectively. It is noted that a polycrystalline sample from batch A was selected because it contains multiple phases. This sample includes not only $PrCdNi_4$ but also impurity phases such as $PrNi_2Cd_{20}$ and $PrNi_5$, which is consistent with the emergence of additional peaks measured by the powder x-ray diffraction shown in Fig. S2. The atomice composition of the $PrCdNi_4$ phase was determined by electron-probe microanalysis (EPMA) to be $Pr_{0.99(1)}Cd_{1.01(1)}Ni_{3.87(3)}$. On the other hand, another sample from batch B is nearly single-phase, but it contains small amounts of $PrNi_5$ and Cd impurities. As shown in Fig. S2, there are some peaks from $PrNi_5$ in the powder x-ray diffraction pattern, although the peaks from $PrNi_2Cd_{20}$ are less pronounced. The composition for the $PrCdNi_4$ phase of sample B was determined to be $Pr_{0.97(1)}Cd_{1.03(1)}Ni_{3.84(6)}$ by EPMA. The compositions of samples A and B are similar to $Pr_{1.00(1)}Cd_{1.00(1)}Ni_{3.89(4)}$ of the sample batch for measurements, and they are close to the stoichiometric ratio compared with $Pr_{0.94(1)}Mg_{1.06(1)}Ni_{3.86(2)}$ in Ref. [1], which shows no phase transition.

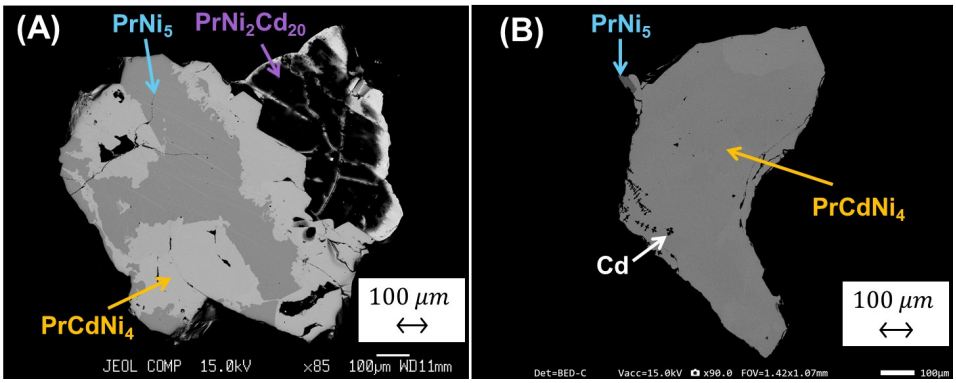

FIG. S1. Backscattered electron images of the samples A and B of $PrCdNi_4$. Sample A contains $PrCdNi_4$ along with impurity phases, such as $PrNi_2Cd_{20}$ and $PrNi_5$, whereas sample B is nearly a single phase.

* kusanose.yuka.p7@f.mail.nagoya-u.ac.jp
† Present address: National Sun Yat-sen University

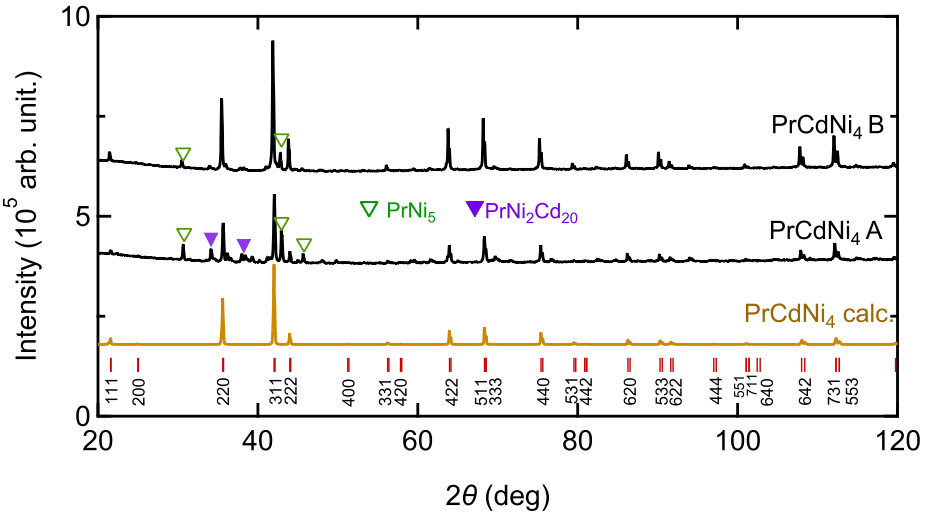

FIG. S2. Powder X-ray diffraction patterns of $PrCdNi_4$ (A) and (B). The lower is the simulated pattern with the cubic $MgSnCu_4$-type structure. Both samples can be indicated by cubic $MgSnCu_4$-type structure, whire additional peaks due to impurity phases shown with triangle.

The impurity phase of $PrNi_5$ was also observed in the powder neutron diffraction pattern at T = 2.0 K, as indicated by a star in Fig. S3. We conducted the Rietveld analysis considering the two phases, $PrCdNi_4$ and $PrNi_5$, and determined their molar ratio to be $PrCdNi_4$:$PrNi_5$ = 98.1(1) : 1.9(1). It is noted that the peaks around 2θ = 64 and 75 deg. were excluded from the analysis because they were due to aluminum from the sample container. Since neutrons can penetrate the samples, this result provides a reasonable stoichiometric ratio for the bulk samples in the macroscopic measurements.

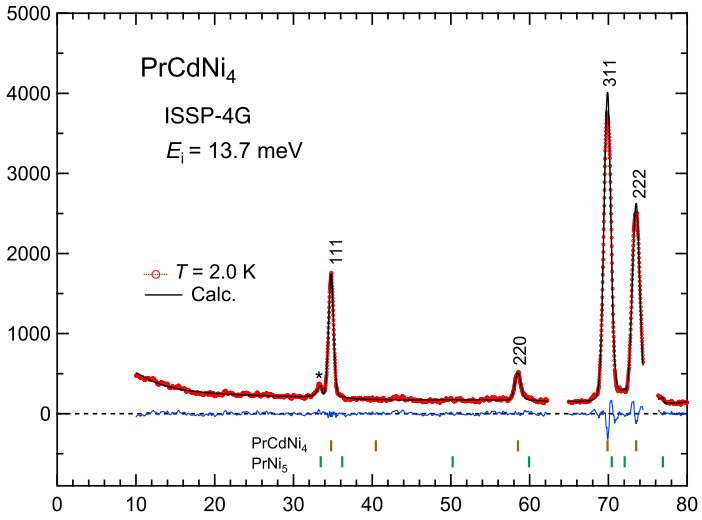

FIG. S3. Powder neutron diffraction patterns of $PrCdNi_4$ at T = 2.0 K. The black line represents the fits to the data with the Rietveld analysis. The blue line shows the difference between the data and calculation. The brown and green bars indicate the scattering angles for the nuclear Bragg peaks of $PrCdNi_4$ and $PrNi_5$.

In Table S1, the structural parameters of $PrCdNi_4$ obtained from the Rietveld profile fitting analysis of neutron powder diffraction patterns for $T = 2.0$ and 0.32 K, shown with the black solid lines in Fig. 7 of the main text, are presented, along with the reliable factors for the fitting. The lattice parameter at 0.32 K decreases by 0.23% compared with the value at 273 K determined by the single-crystal X-ray analysis described in the next section.

Table S1: Structural parameters of $PrCdNi_4$ refined by the Rietveld profile fitting analysis of neutron powder diffraction patterns. The space group is $F\bar{4}3m$ (#216), where the Pr atoms occupy the 4*a* site at (0, 0, 0), the Cd atoms the 4*c* site at (1/4, 1/4, 1/4), and the Ni atoms 16*e* site at (x_{Ni}, x_{Ni}, x_{Ni}) with $Z = 4$.

	0.32 K	2.0 K
Lattice parameters		
a (Å)	7.1112(3)	7.1114(1)
V (Å^3)	359.61(3)	359.644(9)
x_{Ni}	0.6278(4)	0.625(2)
Reliable factor		
R_p	4.74	5.20
R_{wp}	6.24	6.75
R_e	5.40	5.36
S	1.15	1.26

II. SINGLE-CRYSTAL X-RAY STRUCTURAL ANALYSIS

To identify the crystal structure, the single-crystal x-ray structural analysis was performed at 273 K with Mo $K\alpha$ radiation, λ = 0.071073 nm, monochromated by a multilayered confocal mirror using a Bruker APEX-II ULTRA CCD area-detector diffractometer at N-BARD, Hiroshima University. Crystallographic parameters and details for the measurement, data collection, and refinement of the single-crystal X-ray diffraction experiment are described in Tables S2 and S3.

Table S2: Information of the measurement, data collection, and refinement of the single-crystal x-ray diffraction experiment for $PrCdNi_4$.

Crystal system	Cubic $MgSnCu_4$
Space group	$F\bar{4}3m$ (#216)
a (Å)	7.12758(4)
V (Å^3)	362.098(3)
Z	4
Dimensions (mm^3)	$0.21 \times 0.14 \times 0.08$
Temperature (K)	293
Radiation, λ (nm)	Mo-$K\alpha$, 0.071073
2θ range (°)	9.908 – 89.674
μ (mm^{-1})	39.061
Data collection	
Measured reflections	15017
Unique reflections	186
h	$-14 \le h \le 14$
k	$-14 \le k \le 14$
l	$-14 \le l \le 14$
Refinement	
$\Delta_\rho$max/$\Delta_\rho$min (eA^{-3})	1.50/−1.62
GoF	1.257
Reflections/parameters	186/7
R_1	0.0157
wR_2	0.0412

Table S3: Crystallographic parameters for $PrCdNi_4$ determined at 273 K. U_{eq} is the isotropic displacement parameter defined as 1/3 of the trace of the orthogonalized U_{ij} tensor.

Cubic $MgSnCu_4$-type						
Space group: $F\bar{4}3m$ (#216)						
a = 7.12758(4) Å, V = 362.098(3) Å^3, Z = 4						
Atom	Site	x	y	z	Occ.	U_{eq} (Å^2)
Pr	4a	0	0	0	1	0.0071(2)
Cd	4c	0.25	0.25	0.25	1	0.0041(2)
Ni	16e	0.62376(5)	0.62376(5)	0.62376(5)	1	0.0052(2)

III. PHONON CONTRIBUTION TO THE SPECIFIC HEAT

Figure S3 shows the temperature dependence of the specific heat $C(T)$ of $PrCdNi_4$ from 2 K to 300 K. The $C(T)$ data increase with elevating temperatures and approach the Dulong-Petit value of $3nR$ = 149.7 J/K mol, where $n = 6$ is the number of atoms per formula unit and R the gas constant. The inset displays the C/T^3 plots with the logarithmical scale. The C/T^3 data increase on cooling. The (red) solid curve is a fit to the C/T^3 data between 50 and 300 K by adopting the Debye model for acoustic phonon modes [2] with the Debye temperatures of θ_D = 270.7(6) K. Since the acoustic phonon contribution to $C(T)$ is proportional to T^3 at lower temperatures, the calculated C/T^3 curve approaches a constant on cooling below 20 K. Thereby, the difference between the data and the calculated curve for $T < 50$ K is ascribed to the electronic and magnetic contributions due to, respectively, the conduction electrons and the $4f^2$ electrons of the Pr ion. The value of θ_D = 270.7(6) K is lower than that of θ_D = 300.3(6) K for an isostructural $LaMgNi_4$ [1]. This is reasonable because the molecular weight of $PrCdNi_4$ is much heavier than that of $LaMgNi_4$.

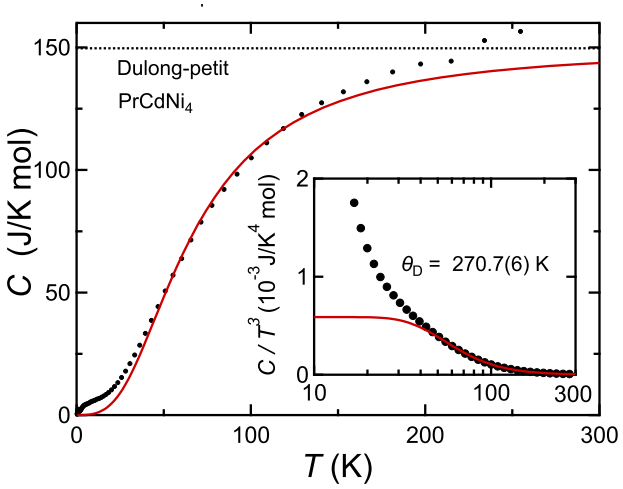

FIG. S4. Temperature variation of the specific heat of $PrCdNi_4$. The inset shows the C/T^3 plot with respect to the logarithmic temperature scale. The (red) solid lines are simulated by adopting the Debye model with a Debye temperature of θ_D = 270.7(6) K.

[1] Y. Kusanose, T. Onimaru, G.B. Park, Y. Yamane, K. Umeo, T. Takabatake, N. Kawata, and T. Mizuta Jpn. J. Phys. Soc. Jpn. **88**, 083703 (2019).

[2] C. Kittel, Introduction to Solid State Physics, 8th ed..,, John wiley & Sons,, 2005, p.112, Chap. 5.